



Calcium signaling is gated by a mechanical threshold in three-dimensional environments

SUBJECT AREAS:
ENGINEERING
BIOPHYSICS
BIOTECHNOLOGY
BIOMATERIALS

Warren C. Ruder¹, Erica D. Pratt^{1,2}, Nailah Z. D. Brandy¹, David A. LaVan³, Philip R. LeDuc^{1,2,4,5} & James F. Antaki^{1,6}

¹Department of Biomedical Engineering, ²Department of Mechanical Engineering, Carnegie Mellon University, 5000 Forbes Avenue, Pittsburgh, PA 15213, ³Material Measurement Laboratory, National Institute of Standards and Technology, 100 Bureau Drive, M/S 8520, Gaithersburg, MD 20899, ⁴Department of Computational Biology, ⁵Department of Biological Sciences, ⁶Department of Computer Science, Carnegie Mellon University, 5000 Forbes Avenue, Pittsburgh, PA 15213.

Received
2 April 2012

Accepted
5 July 2012

Published
3 August 2012

Correspondence and requests for materials should be addressed to P.R.L. (prleduc@cmu.edu) or J.F.A. (antaki@cmu.edu)

Cells interpret their mechanical environment using diverse signaling pathways that affect complex phenotypes. These pathways often interact with ubiquitous 2nd-messengers such as calcium. Understanding mechanically-induced calcium signaling is especially important in fibroblasts, cells that exist in three-dimensional fibrous matrices, sense their mechanical environment, and remodel tissue morphology. Here, we examined calcium signaling in fibroblasts using a minimal-profile, three-dimensional (MP3D) mechanical assay system, and compared responses to those elicited by conventional, two-dimensional magnetic tensile cytometry and substratum stretching. Using the MP3D system, we observed robust mechanically-induced calcium responses that could not be recreated using either two-dimensional technique. Furthermore, we used the MP3D system to identify a critical displacement threshold governing an all-or-nothing mechanically-induced calcium response. We believe these findings significantly increase our understanding of the critical role of calcium signaling in cells in three-dimensional environments with broad implications in development and disease.

The significant influence of the three-dimensional cellular milieu on cell physiology is widely appreciated in many fields including biomaterials, tissue engineering, and cell biology. Our understanding of a range of cellular behaviors and the dynamics of spatiotemporal cell signaling has been enhanced by analysis in experimental systems that recreate *in vivo* environments where cells respond to an diverse range of extracellular environmental cues including mechanics, scaffolding, electrical potential, and biochemical agonists. For example, local mechanical stresses are processed into intracellular biochemical events affecting multiple cell behaviors including tissue and extracellular matrix (ECM) remodeling, cytoskeletal restructuring, gene transcription, metabolism, differentiation, and motility^{1–4}. Much of this mechanotransduction process is believed to originate at the focal adhesion complex (FAC), where integrin receptors on a cell's surface bind to ligands in the ECM and translate extracellular mechanical events into intracellular biochemical signals^{1,2,5}. If this mechanochemical interface is impaired, resulting deficiencies in cellular mechanosensation can have affect pathologies ranging from cardiopulmonary disease to deafness^{1,6}.

Experimental studies of biomechanics conducted *in vitro* must therefore include prescribed mechanical boundary conditions and cellular ECM structure^{2,7}, both of which play key roles in mechanotransduction⁸. Conversely, assaying biomechanical cellular events can be confounded by limitations in current 2D cell culture and imaging techniques. Most of these *in vitro* studies of cell function occur on 2D-constrained planar glass or polymer surfaces, including studies that use optical tweezers, magnetic needles, or flexible substrates. Yet, physiological environments are almost always 3D. For example, fibroblasts adopt a stellate morphology in tissue or ECM gels, but dramatically spread and form a lamellar structure with a raised nuclear bulge when cultured on 2D substrate⁹. It has been shown that NIH 3T3 fibroblasts cultured between a micron-gap polyacrylamide bilayer materials system, providing both dorsal (on the cell's upper surface) attachment points as well as ventral (on the cell's lower surface) attachments, allowed for more physiological morphologies to be observed *in vitro*⁹.

These previous studies motivated the development of the MP3D system¹⁰ shown in Fig. 1, a new experimental approach that allows for carefully prescribed mechanical perturbation. It also provides access to the cell membrane for perfusion with biochemical agonists, allowing for simultaneous mechanical and chemical stimulation of

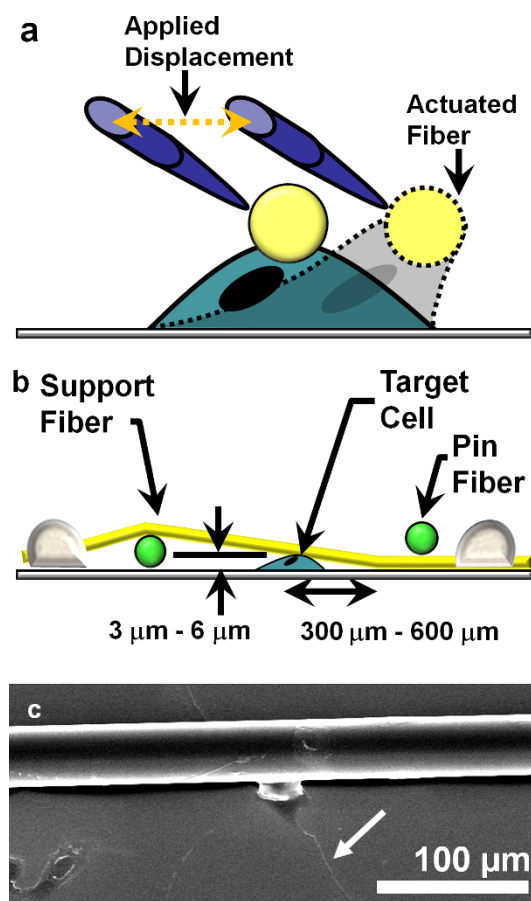


Figure 1 | MP3D culture and imaging platform for probing cellular signal transduction¹⁰. (a) Polypropylene scaffolds erected on glass consisted of microfibers aligned in a crosshair pattern with an *actuated fiber* (yellow) stretched over a central *support fiber* (green) and held against the glass by a *pin fiber* (green). Cells in the system can be mechanically manipulated by actuating the upper fiber with a micromanipulated needle. A micromanipulated needle tip is used to displace the upper fiber, resulting in cell deformation. (b) A side view of the MP3D system shows the gap size for cell attachment can be adjusted by controlling the position of the polypropylene fibers. We targeted a 3 μm to 6 μm gap for dorsal attachment based on the cell height of NIH 3T3s. (c) A scanning electron microscope (SEM) image of a cell cultured in the MP3D device attached to the actuated (horizontal) fiber. The cell extends a long, thin process (white arrow) reminiscent of stellate fibroblasts.

fibroblasts assuming physiological morphologies. We found that cells grown in the system showed altered morphology reminiscent of the stellate cellular morphologies seen in three-dimensional extracellular *in vitro* matrices. These cells altered their cytoskeletal networks in comparison to cells grown on planar glass substrate alone, and robustly increased calcium signaling when mechanically perturbed.

We chose to investigate calcium because it functions as a ubiquitous messenger in cells, regulating processes ranging from fertilization, embryogenesis, muscle contraction, and synaptic vesicle release to gene transcription and metabolism^{7,11,12} as well as the sensing of shear stress by endothelial cells^{13–15}. One 2D approach used to study calcium mechanotransduction has been the application of displacement by stretching the cellular substratum^{16,17}. Alternatively, stimulation of beads attached to integrin receptors on the dorsal surface of cells has been used with some success^{8,18,19}. Typically, polystyrene beads (possibly with magnetic cores) that are coated with the physiological ligand for integrin receptors (proteins containing the R-G-D

peptide sequence such as fibronectin) are bound to the integrin receptors of cells to form physiological attachments^{20,21}. Beads are then trapped with either optical or magnetic tweezers to apply force where attachments have formed. The formation of attachments and associated protein complexes are typically achieved over a span of 10 min to 30 min in these systems, and while they can be physiologically dynamic and are known to occur within this time period, assessing the relevance of dorsal attachments formed over longer periods of time remains a challenge with these techniques.

In the work presented here, we investigated the calcium response during mechanical stimulation followed by traditional chemical stimulation with adenosine triphosphate (ATP), a robust agonist of purinergic (P2Y) receptors that couple directly to endoplasmic reticulum (ER) calcium stores through the $G_{\alpha,q/11}/IP_3$ second-messenger cascade, and then ionomycin. The latter increases membrane calcium permeability and, at supramaximal doses, can cause large, irreversible release of calcium stores, thus providing an upper reference response. In the MP3D system, we previously found that stretching the upper membrane of the cell created a spike in intracellular $[Ca^{2+}]$ similar to the waveform observed following chemical stimulation and here we set out to compare these dynamics to calcium signaling resulting from other mechanical approaches.

Results

To gain further insight into the behavior of the mechanically-induced cellular calcium responses, we explored calcium signaling in response to two techniques widely used in mechanotransduction studies^{17,18}. First, we monitored cells in response to substratum stretch by growing cells on low stiffness, flexible PDMS substrates (Fig. 2, Supplementary Videos 1 and 2). Second, we monitored calcium response to stress using magnetic tensile cytometry (MTC), an approach that uses supermalloy-core, water-cooled electromagnetic needles to expose paramagnetic beads on cell surfaces to high (nN) force, which is significantly higher than the pN range of magnetic or optical tweezers. These experiments are detailed in Fig. 3 and S1 as well as Supplementary Videos 3 and 4. With both of these techniques, mechanical force and displacement were provided for durations longer than that required for calcium firing to occur following either chemical or MP3D-based mechanical stimuli. Nevertheless, in both cases, despite significant force and displacement, the calcium response was minimal or unapparent, in comparison to control stimulus with ATP or ionomycin.

We next used the MP3D system to prescribe tightly-controlled, stepwise displacement to cells and monitored resulting calcium signaling. As noted in Fig. 4 and Supplementary Video 5, we gradually increased displacement to the upper fiber until calcium firing occurred. In all cases, after an initial displacement the cell did not present a calcium response. However, upon further stimulation the cell presented a calcium spike that rapidly returned to baseline with a decay rate similar to that following the subsequent stimulus with ATP. These experiments revealed a threshold/trigger point in the calcium response to displacement. This threshold provides mechanistic insight into the gating of calcium signaling in response to stress. At a critical point, stretch becomes significant enough to allow calcium to increase in the cytosol. The presence of this trigger point provides additional mechanistic consistency with a potential calcium signaling model in which MP3D system displacement enables calcium to enter through stretch-activated channels (SACs), and then interface with faster calcium-handling machinery components, a stark comparison to slower responses previously noted in NIH 3T3s¹⁷.

Discussion

By comparing cellular responses elicited by the MP3D system with those resulting from MTC and flexible substrate approaches, new biological insights into cellular mechanotransduction are possible.

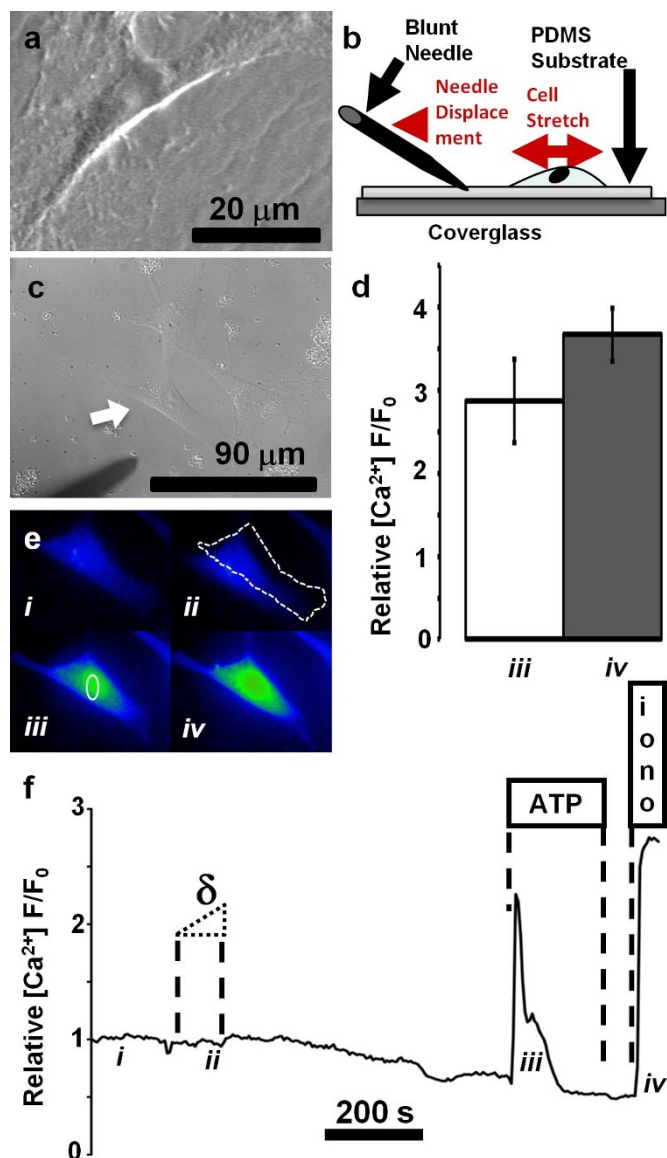


Figure 2 | Flexible substratum stretching deforms NIH 3T3 fibroblasts without mobilizing calcium. (a) SEM image of NIH 3T3s cultured on soft (40:1 ratio of polymer to crosslinker by volume) PDMS substrate. (b) Schematic showing the basic setup for flexible substrate stretching. (c) Differential interference contrast (DIC) image of cells on flexible substrate prior to the application of displacement. (d) Histogram showing the maximum response of cells to 100 μmol/L ATP, a purinergic agonist (2.87 ± 0.49 , iii in (e)) and 5 μmol/L ionomycin, a potent ionophore (3.66 ± 0.32 , iv in (e)), as a function of the unitless ratio of fluorescent intensity, F , to initial fluorescent intensity, F_0 . Responses to an increasing displacement, δ , were not observed in any experiments. Data given as mean \pm standard error of the mean ($n = 6$ cells in 3 experiments). (e) Pseudo-color images from a time series of cellular calcium response representing time points before the application of displacement (i), during the application of displacement (ii), during control stimulus with ATP (iii), and with ionomycin (iv). (f) Time course of the normalized fluorescent intensity (F/F_0) in the ROI (white oval in Fig. 2e, iii) from the cell proximal to the needle tip (white arrow in Fig. 2c). Points (i, ii, iii, iv) corresponding to the images in Fig. 2e are noted. The entire fluorescent image series is provided as Supplementary Video 1 with Supplementary Video 2 providing a DIC image series showing the mechanical behavior of the stretched substrate.

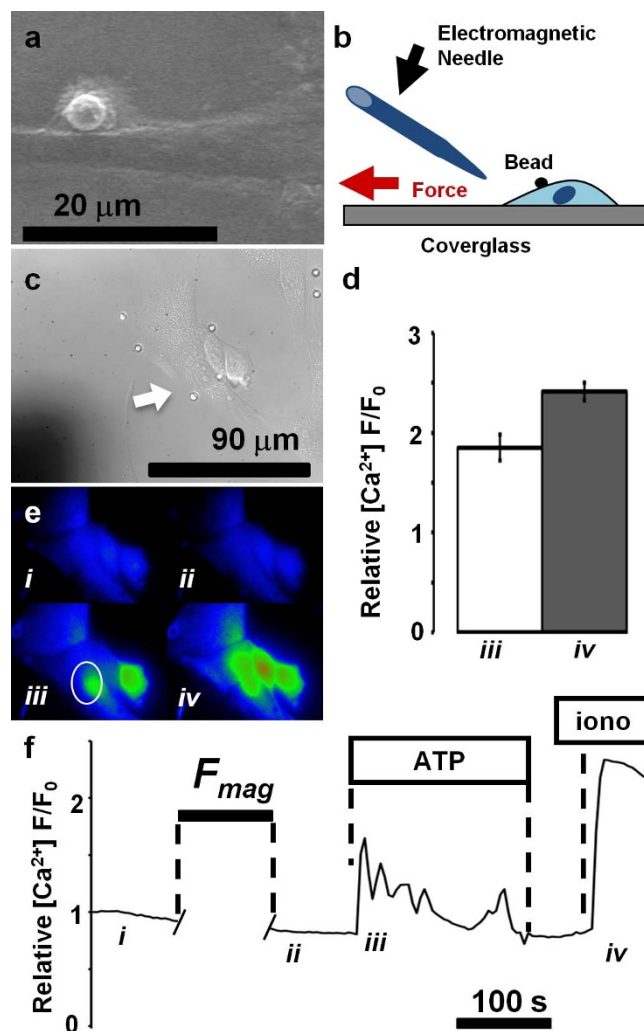


Figure 3 | MTC applies force to NIH 3T3 fibroblasts without mobilizing calcium. (a) SEM image of NIH 3T3 fibroblasts cultured on glass attached to a 4.35 μm diameter paramagnetic bead. (b) Schematic showing the basic setup for MTC, consisting of an electromagnetic tip placed near a cell with a fibronectin-functionalized paramagnetic bead attached to its surface. (c) DIC image of cells with beads prior to the application of magnetic force. (d) Histogram showing the maximum response of cells to 100 μmol/L ATP, a purinergic agonist (1.83 ± 0.13 , iii in (e)) and 5 μmol/L ionomycin, a potent ionophore (2.41 ± 0.09 , iv in (e)), as a function of the ratio of fluorescent intensity, F , to initial fluorescent intensity, F_0 . Responses to force, F_{mag} , were not observed in any experiments. Data given as mean \pm standard error of the mean ($n = 9$ cells in 3 experiments). (e) Pseudo-color images from a time series of cellular calcium response representing time points before the application of force (i), immediately after the application of force (ii), during control stimulus with 100 μmol/L ATP (iii), and with ionomycin (iv). (f) Time course of the normalized fluorescent intensity (F/F_0) from the ROI (white oval in Fig. 3e, iii) in the cell proximal to the magnet tip (white arrow in Fig. 3c). Points (i, ii, iii, iv) corresponding to the images in Fig. 3e are noted. The entire fluorescent image series is provided as Supplementary Video 3 with electromagnetic needle calibration shown in Supplementary Video 4 as a phase contrast microscopy image series. During the application of magnetic force, the halogen lamp is turned on so that the needle position can be observed. As a result, the fluorescent signal is not used for analysis during this period of applied force and an extremely bright background is visible in the image series.

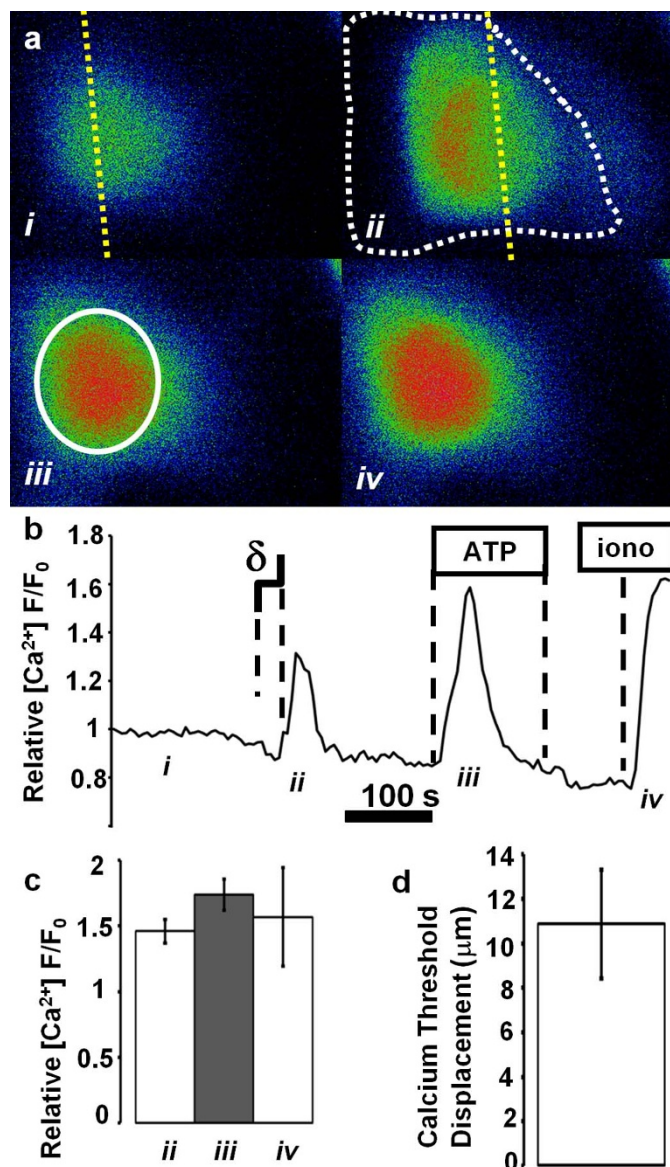


Figure 4 | MP3D mechanical system induces calcium response upon reaching a displacement threshold. (a) Pseudo-color images from a time series of cellular calcium response representing time points before the application of MP3D fiber displacement (i), during the application fiber displacement (ii), during control stimulus with ATP (iii), and with ionomycin (iv). Dotted border shows location of cell prior to the application of displacement, δ . Dotted line shows the leftmost edge of the upper fiber prior to and during maximum displacement. The entire right portion of the cell is overlapped by the fiber. Each image is $35 \mu m \times 47 \mu m$. (b) Time course of the normalized fluorescent intensity (F/F_0) in the ROI defined by the white oval in (a). Points (i, ii, iii, iv) corresponding to the images in Fig. 4a are noted. The entire fluorescent image series is provided as Supplementary Video 5. (c) Histogram showing the maximum response of cells to fiber displacement (1.46 ± 0.09 , ii in (a)), $100 \mu mol/L$ ATP, a purinergic agonist (1.73 ± 0.12 , iii in (a)) and $5 \mu mol/L$ ionomycin, a potent ionophore (1.56 ± 0.37 , iv in (a)), as a function of the ratio of fluorescent intensity, F , to initial fluorescent intensity, F_0 . (d) Histogram showing the threshold for total fiber displacement sufficient to activate calcium ($10.8 \mu m \pm 2.4 \mu m$). Displacement was applied in incremental steps, held 20 s, and then increased if a qualitatively significant response was not observed. This process continued until calcium spiked, always immediately after the application of the final displacement step, at which point the displacement was removed. No cell required more than a third step. Data given as mean \pm standard error of the mean ($n = 4$ cells in 3 experiments).

For example, in a previous study, the use of displacement applied through flexible polyacrylamide substrates revealed a persistent increase in NIH 3T3 fibroblast intracellular calcium at 10 min after membrane stretch¹⁷. The displacement stimulus was applied for 5 min, and the results were obtained as either single fluorescent images before stretch or as images taken at 10 min following stretch, without quantitative comparison to controls such as a store-coupled receptor stimulus like ATP or an ionophore like ionomycin. These findings suggest a different mode of calcium activation that may persist beyond the normal time required for calcium extrusion and return to baseline in these cells¹¹. Additionally, this lengthy, persistent calcium response was significantly slower than calcium signaling that results from activation of the canonical store-operated pathway, triggered by G-protein coupled receptors, and required a significantly prolonged application of stimulus. This resulting slow, persistent mode potentially relies on alternate calcium mechanisms operating with a time constant less reminiscent of rapid calcium firing and more reminiscent of protein-protein regulation, perhaps through the interplay of kinases activated by calcium or mechanics.

Similarly, previous MTC experiments revealed spikes in calcium following mechanical stimulation in bovine capillary endothelial cells (BCEs). However, these reported responses peaked between $150 \text{ nmol/L} - 200 \text{ nmol/L}$, while receptor-mediated, store-enhanced calcium responses often reach an order of magnitude greater¹⁸. As shown in Fig. 4, with the MP3D system, we observed calcium responses of comparable magnitude to chemical activation through receptor-mediated calcium release.

The MP3D system provides added advantages over bead-based assays by bearing stress during cell attachment formation. In typical bead-based studies, the ligand-conjugated beads are allowed to settle onto cell surfaces, where cell receptors bind to the ligand^{18,19,21}. However, during the formation of physiological attachments, as actin polymerization occurs intracellularly, tethering the cytoskeleton to intracellular components, the cell will exert force against its environment. Compared to beads on the dorsal surface, which provide a limited ability to support tensile stress, in the MP3D ligand-coated fibrous system, this stress is maintained over a period of time necessary for gene transcription and translation to occur (hours to days) through both ventral and dorsal attachments. Matrix stiffness has been shown to be a major determinant of the phenotype and homeostatic maintenance of signaling in individual cells^{3,4,22,23}, indicating that the stress bearing capacity of the MP3D environment used here could be critical.

We believe that a potentially overlooked aspect of a fibroblast's capacity to interpret local mechanical cues is this ability to support stress (in addition to its ability to sense matrix stiffness). In many 2D experiments, a flexible substrate with high stiffness will allow greater tension to be supported by a fibroblast's actin stress fiber network, whereas a more compliant substrate will support less tension. However, fibroblasts exist in 3D matrices that they actively remodel – a process with significant pathological implications, for example, in heart disease²⁴. In the case of cardiac remodeling and hypertrophy, prior to the initiation of pathological remodeling, fibroblasts sense 3D stress profiles in healthy, more compliant ECM and dynamically maintain the tissue's mechanical homeostasis²⁴. Following the initiation of disease, some fibroblasts differentiate into myofibroblasts and pathologically remodel the heart, resulting in fibrosis and increases in stiffness. During normal homeostasis, a combination of factors beyond matrix stiffness alone²⁴ drives fibroblast behavior. In our work here, the more physiological morphologies we observed in relatively rigid materials speaks to the importance of 3D spatial anchoring points that can bear stress in comparison to bead-based assays.

For example, taking into account the tendency of SACs to accrue at the leading edge of motile NIH 3T3s¹⁷, also a region of increased cytoskeletal and FAC protein abundance, we believe that the



geometrical confines of the MP3D system provide an environment where cells, adopting a more *in vivo* morphology, accrue cytoskeletal and FAC proteins dorsally in addition to ventrally, possibly along with SACs. As a result, after ventral surface bead deflections, the overall number of channels activated may be enough to increase calcium entry in 2D-cultured endothelial cells such as BCEs, but may not be enough to mobilize other calcium modulating mechanisms. However, application of displacement using the MP3D system, which is connected to the entire cytoskeleton through a mature cytoskeletal network, may be more effective in mobilizing calcium in stromal cell types.

Both in the case of substratum stretching and MTC, observations of seemingly different or absent calcium signaling illustrate the necessity of approaches for probing these responses. Moreover, the observation of a strong calcium response in NIH 3T3s using the MP3D system suggests that mechanically-induced calcium signaling is especially complicated, regulated by both the endogenous calcium-binding proteins involved in other forms of calcium signaling, as well as those activated specifically by FACs. This is especially evident in our observations of a mechanical threshold that gates calcium signaling following the application of displacement. As noted, robust intracellular calcium signaling throughout the cytosol was only observed following the application of a final mechanical stimulus step when applying displacement in a stepwise fashion. Rather than a gradual increase in intracellular calcium as displacement is increased – a result that might be expected if the rise in intracellular calcium resulted solely from influx through SACs – it appears likely that multiple calcium pathway components are involved in setting a threshold for mechanically-induced calcium signaling in three-dimensional environments. Ultimately, these results highlight the importance of the biophysical and biochemical environment in cell physiology as well as the necessity of exploring the interplay of signaling arising from mechanical and chemical stimuli.

Methods

MP3D device construction. MP3D devices were constructed as previously described¹⁰. Briefly, melted polypropylene was drawn manually to form microfibers (25 μm to 50 μm radius) and stacked perpendicularly (2 fibers high) on #1 borosilicate glass coverslides (22 mm \times 40 mm), resulting in a variable gap between the substrate and the uppermost fiber (Fig. 1). PDMS (Sylgard 184, Dow Corning) droplets were used to secure fibers in place. MP3D devices were sterilized in 70 % ethanol, rinsed in phosphate buffered saline (PBS), and incubated (1 h) in 20 $\mu\text{g}/\text{mL}$ fibronectin to promote cell attachment.

Cell culture. NIH/3T3 fibroblasts (ATCC, CRL-1658TM) were cultured in high glucose Dulbecco's modified Eagle's medium (DMEM) supplemented with 10 % bovine calf serum and 1 % GPS solution (29.2 mg/mL L-glutamine, 6 $\mu\text{g}/\text{mL}$ (10 U/mL) penicillin, and 10 $\mu\text{g}/\text{mL}$ streptomycin). Cells were maintained in a humidified incubator at 37 °C with 5 % CO₂. Fibroblasts were plated onto sterilized MP3D devices and grown overnight. Cells were subcultured according to ATCC protocols and were never allowed to become more than 80 % confluent. Cells were maintained using a subcultivation ratio of 3×10^3 cells/cm² to 5×10^3 cells/cm². MP3D devices were seeded at the same density and used for experiments 24 h to 48 h later.

MP3D device imaging. MP3D devices¹⁰ were mounted in an open-bath perfusion chamber (Series 20, Warner Instruments) and bathed in Ringer's solution containing: 121 mmol/L NaCl, 2.4 mmol/L K₂HPO₄, 0.4 mmol/L KH₂PO₄, 1.2 mmol/L CaCl₂, 1.2 mmol/L MgCl₂, 5.5 mmol/L glucose, and 10 mmol/L Hepes titrated to pH 7.4 by incrementally adding 1 mol/L NaOH. The MP3D device and bath assembly was mounted on the stage of an inverted, epifluorescent optical microscope (Zeiss Axiovert 200) equipped with both halogen and 100 W mercury arc light sources, a computer-controlled shutter (Sutter), and a fluorescent filter set (450 nm to 490 nm bandpass excitation, 510 nm beam splitter, 515 nm to 565 nm bandpass emission). A precision (0.8 μm degree⁻¹) micromanipulator (Newport Instruments) was used to position a needle probe (tip radius < 40 μm) to displace individual polymers. Images were captured by a CCD camera (Insight QE, SPOT Imaging Solutions), and images were post-processed using NIH ImageJ software.

Fluorescent calcium imaging. Prior to calcium imaging, MP3D devices were incubated with 2 $\mu\text{mol}/\text{L}$ Fluo-4-AM calcium dye for 30 min and then mounted as described above. Cells were exposed for 150 ms to mercury arc light every 5 s and fluorescent emission was captured. During chemical stimulation, a Ringer's solution containing either 100 $\mu\text{mol}/\text{L}$ ATP or 5 $\mu\text{mol}/\text{L}$ ionomycin was continually superfused until the chamber volume was exchanged.

Flexible substrate experiments. Soft substrates were prepared by spreading a reduced ratio (40:1) solution of PDMS (Sylgard® 184) polymer to crosslinker on #1 borosilicate glass coverslips, and then cured overnight as previously described²⁵. We then added 0.5 mL of fibronectin in EtOH (20 $\mu\text{g}/\text{mL}$) to the surface and let the fibronectin deposit through solvent evaporation. A blunt needle tip mounted to a micromanipulator was then pushed downward into the substrate, and moved away from the cell to stretch the cell membrane as illustrated in Fig. 2. Cells were stretched gradually over \approx 60 s to 120 s until the proximal cell edge displaced \approx 10 μm . The elastic modulus of the substrates was approximately 6.5×10^4 N/m² as described previously²⁶. An example of substrate stretching motion is shown as a time series of DIC images in Supplementary Video 2.

Magnetic tensile cytometry. Magnetic tensile cytometry (MTC) was performed using a water-cooled electromagnetic, consisting of a water-jacketed supermalloy core wrapped with 800 turns of 127 μm diameter (36 gauge) varnish-insulated copper magnet wire (McMaster-Carr)²⁷. The magnetic core consisted of supermalloy/HyMU-80, consisting of 80 % Ni, 4.9 % Mo, and 15 % Fe (0.1 % trace impurities) (National Electronic Alloys) with a maximum permeability, μ_{max} , of 229,000 H/m. The coil resistance was 13.7 Ω . During MTC experiments, the needle tip was placed at least 400 μm away from targeted cells. Immediately prior to tests, ice water was flowed through the system, power was provided to the coil until any thermally-induced needle volume changes stabilized, and the current stabilized at 1 A. The needle tip was then brought near (\approx 20 μm) the cells of interest to apply magnetic force. In preparation for MTC-calcium experiments, in the last 10 min of Fluo-4-AM loading, cells were treated with fibronectin-functionalized 4.35 μm paramagnetic beads (Spherotech). Cells treated with beads were then washed with Ringer's solution. The setup is shown in Figs. 3 and S1. Further details can be found in the Supplementary Information.

1. Ingber, D. E. Mechanobiology and diseases of mechanotransduction. *Ann. Med.* **35**, 564–577 (2003).
2. Vogel, V. & Sheetz, M. Local force and geometry sensing regulate cell functions. *Nat. Rev. Mol. Cell Biol.* **7**, 265–275 (2006).
3. Engler, A. J., Sen, S., Sweeney, H. L. & Discher, D. E. Matrix elasticity directs stem cell lineage specification. *Cell* **126**, 677–689 (2006).
4. Engler, A. J., Sweeney, H. L., Discher, D. E. & Schwarzbauer, J. E. Extracellular matrix elasticity directs stem cell differentiation. *J. Musculoskelet. Neuronal Interact.* **7**, 335 (2007).
5. Lee, J., Ishihara, A., Oxford, G., Johnson, B. & Jacobson, K. Regulation of cell movement is mediated by stretch-activated calcium channels. *Nature* **400**, 382–386 (1999).
6. Sussman, M. A., McCulloch, A. & Borg, T. K. Dance band on the Titanic: biomechanical signaling in cardiac hypertrophy. *Circ. Res.* **91**, 888–898 (2002).
7. Carafoli, E. Calcium signaling: a tale for all seasons. *Proc. Natl. Acad. Sci. USA* **99**, 1115–1122 (2002).
8. Wang, N., Butler, J. P. & Ingber, D. E. Mechanotransduction across the cell surface and through the cytoskeleton. *Science* **260**, 1124–1127 (1993).
9. Beningo, K. A., Dembo, M. & Wang, Y. L. Responses of fibroblasts to anchorage of dorsal extracellular matrix receptors. *Proc. Natl. Acad. Sci. USA* **101**, 18024–18029 (2004).
10. Ruder, W. C. *et al.* Three-dimensional microfiber devices that mimic physiological environments to probe cell mechanics and signaling. *Lab Chip* **12**, 1775–1779 (2012).
11. Berridge, M. J., Bootman, M. D. & Roderick, H. L. Calcium signalling: dynamics, homeostasis and remodelling. *Nat. Rev. Mol. Cell Biol.* **4**, 517–529 (2003).
12. Berridge, M. J., Lipp, P. & Bootman, M. D. The versatility and universality of calcium signalling. *Nat. Rev. Mol. Cell Biol.* **1**, 11–21 (2000).
13. Kwan, H. Y., Leung, P. C., Huang, Y. & Yao, X. Depletion of intracellular Ca²⁺ stores sensitizes the flow-induced Ca²⁺ influx in rat endothelial cells. *Circ. Res.* **92**, 286–292 (2003).
14. Li, Y. S., Haga, J. H. & Chien, S. Molecular basis of the effects of shear stress on vascular endothelial cells. *J. Biomech.* **38**, 1949–1971 (2005).
15. Miyazaki, T., Honda, K. & Ohata, H. Requirement of Ca²⁺ influx- and phosphatidylinositol 3-kinase-mediated m-calpain activity for shear stress-induced endothelial cell polarity. *Am. J. Physiol. Cell Physiol.* **293**, C1216–C1225 (2007).
16. Kubicek, J. D., Brelsford, S., Ahluwalia, P. & Leduc, P. R. Integrated lithographic membranes and surface adhesion chemistry for three-dimensional cellular stimulation. *Journal of Biomechanics* **42**(2), 187–192 (2009).
17. Munevar, S., Wang, Y. L. & Dembo, M. Regulation of mechanical interactions between fibroblasts and the substratum by stretch-activated Ca²⁺ entry. *J. Cell Sci.* **117**, 85–92 (2004).
18. Matthews, B. D., Overby, D. R., Mannix, R. & Ingber, D. E. Cellular adaptation to mechanical stress: role of integrins, Rho, cytoskeletal tension and mechanosensitive ion channels. *J. Cell Sci.* **119**, 508–518 (2006).
19. Wang, Y. *et al.* Visualizing the mechanical activation of Src. *Nature* **434**, 1040–1045 (2005).
20. Wang, Y. *et al.* Integrins regulate VE-cadherin and catenins: dependence of this regulation on Src, but not on Ras. *Proc. Natl. Acad. Sci. USA* **103**, 1774–1779 (2006).



21. Meyer, C. J. *et al.* Mechanical control of cyclic AMP signalling and gene transcription through integrins. *Nat. Cell Biol.* **2**, 666–668 (2000).
22. Griffith, L. G. & Swartz, M. A. Capturing complex 3D tissue physiology in vitro. *Nat. Rev. Mol. Cell Biol.* **7**, 211–224 (2006).
23. Zaman, M. H. *et al.* Migration of tumor cells in 3D matrices is governed by matrix stiffness along with cell-matrix adhesion and proteolysis. *Proc. Natl. Acad. Sci. USA* **103**, 10889–10894 (2006).
24. Souders, C. A., Bowers, S. L. & Baudino, T. A. Cardiac fibroblast: the renaissance cell. *Circ. Res.* **105**, 1164–1176 (2009).
25. Cheng, C. M. *et al.* Probing localized neural mechanotransduction through surface-modified elastomeric matrices and electrophysiology. *Nat. Protoc.* **5**, 714–724 (2010).
26. Cheng, C.-M. & LeDuc, P. R. Creating cellular and molecular patterns via gravitational force with liquid droplets. *Appl. Phys. Lett.* **93**, 174106 (2008).
27. Matthews, B. D., LaVan, D. A., Overby, D. R., Karavitis, J. & Ingber, D. E. Electromagnetic needles with submicron pole tip radii for nanomanipulation of biomolecules and living cells. *Appl. Phys. Lett.* **85**, 2968–2970 (2004).

Acknowledgements

The authors thank Professor C.M. Cheng for technical assistance with SEM imaging. This work was supported in part by the National Science Foundation (CMMI-0856187 and CMMI-1160840) and the Office of Naval Research (N000140910215). W.C.R. was supported by a Dowd-ICES predoctoral fellowship awarded by CMU as well as by the

NIH-NIBIB training grant T32 EB0003392 entitled 'Biomechanics in Regenerative Medicine'. E.D.P. and N.Z.D.B. were supported in part by a REU supplement to NSF grant EF-0331657 at the CMU Center for Bioimage Informatics. Certain commercial equipment, instruments, or materials are identified in this document. Such identification does not imply recommendation or endorsement by the National Institute of Standards and Technology, nor does it imply that the products identified are necessarily the best available for the purpose.

Author contributions

W.C.R., D.A.L., P.R.L., and J.F.A. designed the study. W.C.R., E.D.P. and N.Z.D.B. performed experiments. W.C.R., P.R.L., and J.F.A. wrote the paper.

Additional information

Supplementary information accompanies this paper at <http://www.nature.com/scientificreports>

Competing financial interests: The authors declare no competing financial interests.

License: This work is licensed under a Creative Commons Attribution-NonCommercial-NoDerivative Works 3.0 Unported License. To view a copy of this license, visit <http://creativecommons.org/licenses/by-nc-nd/3.0/>

How to cite this article: Ruder, W.C. *et al.* Calcium signaling is gated by a mechanical threshold in three-dimensional environments. *Sci. Rep.* **2**, 554; DOI:10.1038/srep00554 (2012).